Charge fluctuations and image potential at oxide-metal interfaces

S. Altieri,[1,2] L. H. Tjeng,[1,3] F. C. Voogt,[4] T. Hibma,[4] O. Rogojanu,[1] and G. A. Sawatzky[1,5]
[1]*Solid State Physics Laboratory, Materials Science Centre, University of Groningen, Nijenborgh 4, 9747 AG Groningen, The Netherlands*
[2]*INFM-National Center on Nanostructures and Biosystems at Surfaces* (S^3), *via G. Campi 213/a, I-41100 Modena, Italy*
[3]*II. Physikalisches Institut, Universität zu Köln, Zülpicher Straße 77, 50937 Köln, Germany*
[4]*Chemical Physics Laboratory, Materials Science Centre, University of Groningen, Nijenborgh 4, 9747 AG Groningen, The Netherlands*
[5]*Department of Physics and Astronomy, University of British Columbia, 6224 Agricultural Road, Vancouver, British Columbia, Canada V6T 1Z1*

(Received 3 June 2002; published 31 October 2002)

We analyze the dynamical response of the Ag metal surface to electronic excitations in a MgO(100)/Ag(100) oxide-metal interface system. *Intrinsic* and *extrinsic* surface plasmon excitations are discussed in relation to mutual interactions between the oxide and the metal. A direct relationship is established between the reduction of charge fluctuation energies in the MgO(100) layers and the image charge screening by the Ag(100) metal surface.

DOI: 10.1103/PhysRevB.66.155432 PACS number(s): 73.20.Mf, 77.55.+f, 79.20.Fv, 79.60.Dp

I. INTRODUCTION

In the last decade, there has been an increasing amount of effort[1–10] to understand theoretically the properties of oxide-metal interfaces. Far away from the interface, i.e., at distances large compared to the interatomic lattice spacing, it is expected that a continuum dielectric approximation can provide an accurate description for various forms of excitations. Very close to the interface, however, the atomistic nature of the metal surface cannot be neglected anymore. It has been suggested, for instance, that the finite wavelength response of the metal surface due to the existence of a Fermi surface introduces strong deviations from the classical electrodynamics results.[4–10]

An experimental determination of the effective influence of the dielectric boundary on the properties of oxide-metal interfaces and other dielectrically mismatched systems is, therefore, highly desired. Such an information can be obtained in a spectroscopic experiment in which charge excitations are created in a thin film on a metal. This is exemplified in Fig. 1 showing a charge fluctuation in which one electron is first removed from one atom and then added onto another atom far away within a thin film on a metal. The energy cost for this excitation (E) in the vicinity of the metal surface will be effectively reduced by $2E_{image}$ with respect to the value (E_o) expected in the absence of the metal surface. Here, E_{image} is the interaction energy of the created charge with its image charge appearing below the metal surface.

In a recent paper,[11] we reported a spectroscopic investigation of ultrathin MgO(100) films epitaxially grown on a Ag(100) substrate. Because of its closed shell electronic structure, MgO allows for a direct determination of various charge fluctuation energies, via a combined x-ray photoemission (XPS) and Auger electron spectroscopy (AES) experiment.[11–13] From these experiments we found that the Coulomb and charge transfer energies in the oxide film are reduced from their bulk values by as much as 1.8 and 2.5 eV, respectively. These large energy reductions were interpreted as being the result of a very efficient screening by the nearby metallic substrate. The use of such efficient image charge screening may provide a method to alter various transition temperatures and properties of correlated oxides.

In the present paper we use electron energy-loss spectroscopy (EELS), XPS, and AES to investigate the dynamical response of the Ag(100) metal surface to electronic excitations occurring in the supported MgO(100) thin films. *Intrinsic* and *extrinsic* surface-plasmon excitations are discussed in relation to mutual interactions between the oxide and the metal.

II. EXPERIMENT

The experiments were carried out in an electron spectrometer described previously.[11] In the XPS and Auger experiments, the electrons were excited with monochromatized Al K_α source ($h\nu = 1486.6$ eV) and were collected at a take-off angle of 55° with respect to the surface normal of the samples. The overall energy resolution of the XPS and Auger experiment is 0.75 eV and 0.5 eV, respectively, as determined using the Fermi cutoff of a Ag reference sample, which was also taken as the zero of the XPS binding energy and the Auger kinetic energy scale. In the EELS experiments, the excitation electrons impinged on the surface

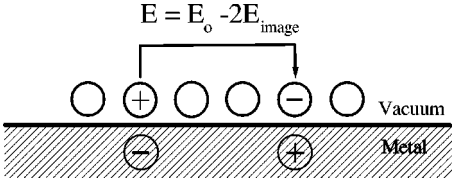

FIG. 1. Charge fluctuation in which one electron is first removed from one atom and then added onto another atom far away within a thin film on a metal. The energy cost for this excitation (E) is effectively reduced by $2E_{image}$ with respect to the value (E_o) expected in the absence of the metal surface. E_{image} is the interaction energy of the created charge with its image charge appearing below the metal surface.

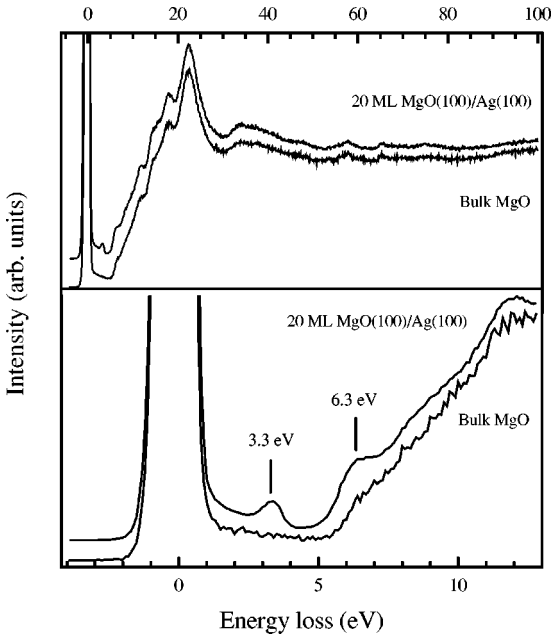

FIG. 2. EELS spectra of 20 ML MgO(100) on Ag(100) (upper curve) and bulk MgO(100) (lower curve), excited with $E_p = 400$ eV. The top panel shows the wide range and the bottom panel the band gap region. The peak at 3.3 eV is due to excitations occurring in the Ag substrate whereas the feature at 6.3 eV corresponds to the surface band gap of MgO.

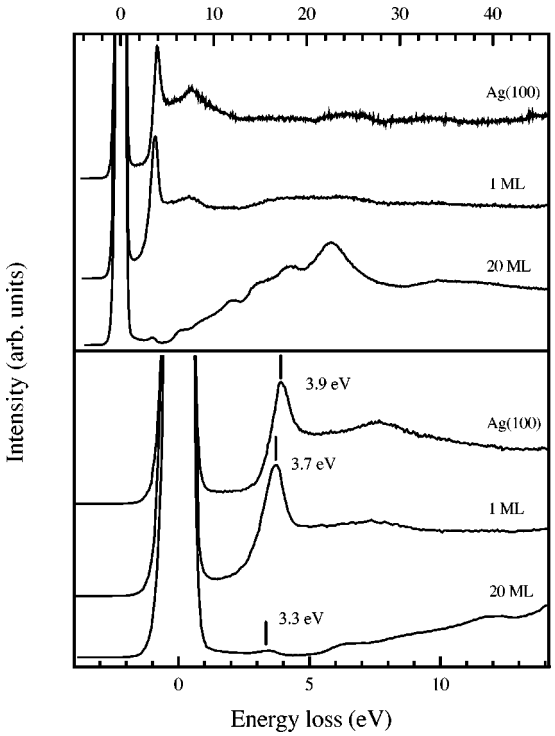

FIG. 3. EELS spectra of clean Ag(100) surface (upper curve), 1 ML MgO(100) on Ag(100) (middle curve), and 20 ML MgO(100) on Ag(100) (lower curve), excited with $E_p = 400$ eV, and normalized in elastic peak height. The top panel shows the wide range and the bottom panel the band gap region. The 3.9 eV Ag(100) surface plasmon peak shifts to 3.7 eV and 3.3 eV when the surface is covered with 1 ML and 20 ML of MgO(100), respectively.

sample at 45°, while the scattered electrons were collected along the surface normal.

Stoichiometric and epitaxial MgO(100) thin films were grown *in situ* as described earlier[11] by evaporating high purity Mg metal from a Luxel Radak-I effusion cell onto a clean and ordered Ag(100) surface, and simultaneously dosing molecular oxygen from a nozzle.

III. RESULTS

Figure 2 shows the EELS spectrum for a 20 ML MgO(100) film on the Ag(100) substrate together with the spectrum for the bulk MgO sample, excited with $E_p = 400$ eV. Strong similarities between the two spectra can be observed in the wide scan shown in the top panel, demonstrating the good chemical and structural quality of the MgO(100) thin films. All of the most important MgO bulk and surface electronic excitations are clearly distinguishable.[14,15] The structures at energies higher than ≈ 51 eV arise predominantly from intraionic transitions on the Mg^{2+} ions involving the Mg $2p$ core level: the peaks at 58 eV and 65 eV can be attributed to $2p \rightarrow 3p$ and $2p \rightarrow 3d$ excitations. At lower energies, the EELS is dominated by the O bulk plasmon peak at 22.4 eV, which corresponds to collective oscillations of the electrons in the O $2p$ valence band. Other peaks appearing at 12 eV, 14 eV, 18 eV, and 34 eV have been assigned to O intraionic and O-to-Mg interionic transitions.[15,16]

The bottom panel of Fig. 2 shows in detail the low energy region of the EELS spectra. This region is most relevant for our study, since it covers the band gap of the MgO bulk, surface, and thin films. A peak at 6.3 eV with a threshold around 5.5 eV can be clearly observed for both the overlayer and the bulk samples. This structure can be ascribed to excitations across the band gap of the surface layer,[14,15,17,18] which is about 2 eV smaller than the bulk band gap [7.8 eV (Ref. 16)] due to the reduced Madelung potential at the surface. In EELS experiments realized under less surface sensitive conditions by tuning E_p from 400 eV to 1600 eV, the intensity of the surface peak is strongly depressed as already reported in earlier studies for a cleaved single crystal.[15] The spectrum of the 20 ML MgO(100)/Ag(100) also exhibits a peak at 3.3 eV, which is totally absent in the spectrum of the bulk sample. At $E_p = 1600$ eV the amplitude of this structure increases by more than a factor of 3, suggesting an origin located either in deep layers of the MgO film or in the metal substrate. It is interesting to note that the EELS spectra from several UHV cleaved MgO(100) single crystals show a prominent peak at 2.3 eV from the zero loss line. This peak has been attributed to the presence of surface defects and can have an amplitude of about 30 50 % of the 6.3 eV surface absorption threshold.[15,19,20] Such a peak is, however, not observed in our thin films of MgO(100) on Ag(100). Perhaps it may lie buried below the 3.3 eV surface plasmon peak of Ag, but if so, then the intensity should be quite low. All in all, this indicates that the crystalline purity of the epitaxially grown 20 ML thick MgO(100) film is much better than that

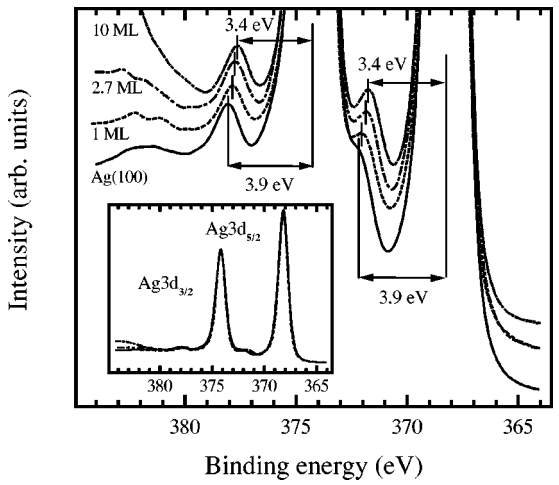

FIG. 4. Ag $3d$ core level XPS spectra of the clean and the MgO(100) covered Ag(100) surface. The main panel shows an enlargement of the spectra depicted in the inset. The clean Ag(100) surface plasmon peak, located at 3.9 eV from both the Ag $3d_{3/2}$ and the Ag $3d_{5/2}$ lines, decreases in energy to 3.7 eV, 3.6 eV, and 3.4 eV when the surface is covered with 1 ML, 2.7 ML, and 10 ML of MgO(100), respectively.

of the reported *in situ* cleaved single crystals. Similar observations have also been made using MgO(100) thin films epitaxially grown on Mo(100) surfaces.[18]

Figure 3 compares the spectrum from the 20 ML MgO(100) film with those from a clean Ag(100) surface and from a surface covered with 1 ML MgO(100), excited with $E_p = 400$ eV. It can be clearly seen that the peak now becomes much larger, by more than one order of magnitude. We thus can assign the 3.3 eV peak to electronic excitations in the Ag metal substrate. From the bottom panel of Fig. 3 it can also be seen that in going from the clean to the monolayer covered metal surface the Ag plasmon peak not only shifts but also broadens by about 0.5 eV to lower energy, partly filling the gap that separated it from the elastic peak. Since the Ag plasmon energy is determined by the interband transition threshold corresponding to the energy position of the Ag $4d$ states with respect to the Fermi level,[21,22] the plasmon peak broadening may signal a modification of the Ag surface states due to the presence of the O $2p$ orbitals.[23]

Figure 4 shows the Ag $3d$ core level XPS spectra of the clean and the MgO(100) covered Ag(100) surface. In the pure Ag a satellite structure is found at 3.9 eV higher binding energy from both the Ag $3d_{3/2}$ and Ag $3d_{5/2}$ due to a plasmon excitation coupled to an interband transition.[21,22] The characteristic energy of this electronic excitation is modified by the ionic overlayers of increasing thickness, going from 3.9 eV in the clean Ag(100), to 3.7 eV, 3.6 eV, and 3.4 eV in the Ag(100) covered with 1 ML, 2.7 ML, and 10 ML of MgO(100), respectively. As summarized in Table I, these XPS satellite energies show an excellent correspondence with the energies of the EELS features of Fig. 3, indicating a common origin, namely, the surface plasmon of the Ag substrate.

In Figs. 5 and 6 we report the Mg $1s$ XPS and Mg $KL_{23}L_{23}$ Auger spectral distribution over an extended energy range far from threshold, from the 1 ML and 20 ML thick films. Especially between 1306 eV and 1314 eV binding energies, there is an appreciable photoemission intensity for the 1 ML film, which instead is almost absent for the 20 ML case (Fig. 5). Part of this extra intensity is concentrated in peak A, which is the 3.7–eV plasmon as discussed above. Perhaps multiple plasmon excitations may also contribute. It is tempting to interpret the energies of the weak features at 7.5 eV (peak B) and 11 eV (peak C) from the main line as being two and three times, respectively, the 3.7 eV plasmon energy. In fact, support for this interpretation can be found from the Mg $KL_{23}L_{23}$ Auger spectrum of the 1 ML film as shown in Fig. 6. Also here, in comparison to the the spectrum of the 20-ML film, there is an extra intensity in the kinetic energy region between the Mg $2p$ two-hole ^1D and ^1S final state peaks, and extra structures on the low kinetic energy side of the ^1S peak. Especially the energies of these extra structures, namely, at 7.5 eV (peak B), 11.5 eV (peak C), and 15.5 eV (peak D) from the ^1D main line, can be expressed quite well in terms of two, three, and four times, respectively, the 3.7 eV plasmon energy.

TABLE I. XPS core level binding energies and Auger electron kinetic energies, together with the intrinsic [$\hbar\omega_s$ (XPS/Auger)] and extrinsic [$\hbar\omega_s$ (EELS)] Ag surface plasmon energies for the clean Ag(100) surface, the 1 ML, 2.7 ML, 10 ML, and 20 ML MgO(100) thin films on Ag(100). All values are in eV.

	Ag(100)	1 ML	2.7 ML	10 ML	20 ML
Ag $3d_{3/2}$	374.2	374.2	374.2	374.2	374.2
Ag $3d_{5/2}$	368.2	368.2	368.2	368.2	368.2
Ag $3d_{3/2}$ plasmon	378.1	377.9	377.8	377.6	
Ag $3d_{5/2}$ plasmon	372.1	371.9	371.8	371.6	
Mg$1s$		1302.7	1303.2	1303.5	1303.6
Mg$1s$ satellite		1306.4			
Mg $KL_{23}L_{23}(^1D)$		1183.4	1181.9	1181.2	1180.7
Mg $KL_{23}L_{23}(^1S)$		1178.4	1176.9	1176.2	1175.7
Mg $KL_{23}L_{23}(^1D)$ satellite		1179.7			
$\hbar\omega_s$ (XPS/Auger)	3.9	3.7	3.6	3.4	
$\hbar\omega_s$ (EELS)	3.9	3.7			3.3

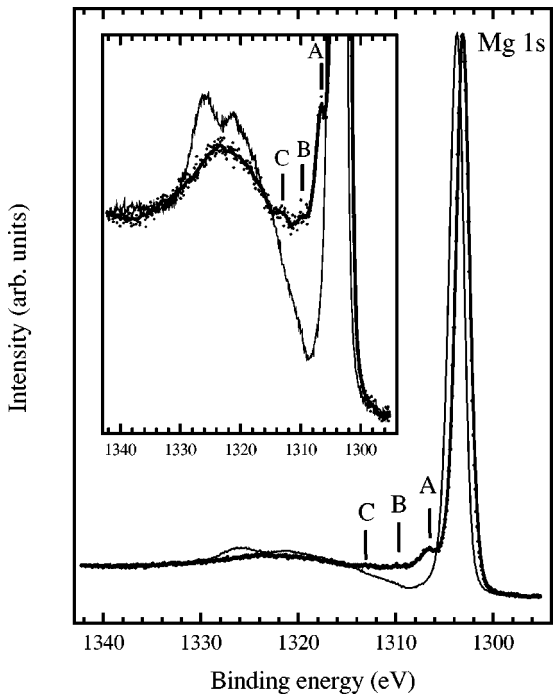

FIG. 5. Mg 1*s* core level XPS spectra of 1 ML (dots, with the thick line as a guide to the eye) and 20 ML (thin line) MgO(100) films on Ag(100). The 20 ML spectrum has been normalized in peak height to the 1 ML spectrum. Features in the 1 ML film, labeled as *A*, *B*, and *C*, absent in the 20 ML film, occur at energies that are higher than the main 1*s* line by multiples of the (reduced) Ag surface plasmon energy. The inset shows a detailed view on these features.

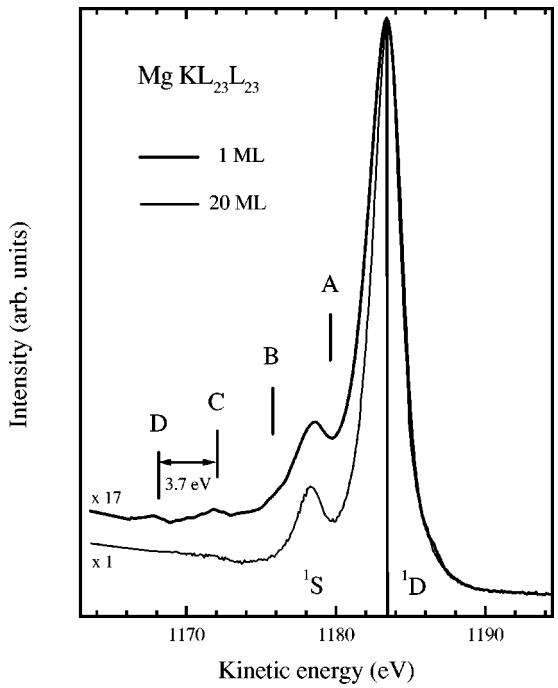

FIG. 6. Mg $KL_{23}L_{23}$ Auger spectra of 1 ML (thick line) and 20 ML (thin line) MgO(100) films on Ag(100). The 20 ML spectrum has been aligned in peak position and normalized in peak height to the 1 ML spectrum. Features in the 1 ML film, labeled as *A*, *B*, *C*, and *D*, absent in the 20 ML film, occur at kinetic energies that are lower than the main ^1D Auger line by multiples of the (reduced) Ag surface plasmon energy.

IV. DISCUSSION

The EELS and the XPS data presented in the preceding section show that the growth of MgO(100) films on a Ag substrate shifts the metal surface plasmon peak to lower energies, due to the formation of the oxide-metal dielectric boundary. This shift is a natural consequence of Maxwell's equations and the boundary conditions at the oxide-metal interface, where the electric field $\vec{E}$ associated with the surface charge density fluctuations is of the same magnitude, but opposite in sign, at opposite sides of the interface. Thus the equation

$$\vec{\nabla}\vec{D}=\vec{\nabla}(\epsilon\vec{E})=\lim_{v\to 0}\left[\frac{1}{v}\int \hat{n}(\epsilon\vec{E})dS\right]=0, \qquad (1)$$

with $\vec{D}$ as the electric displacement vector, and $\hat{n}$ the unit surface normal for a Gaussian pillbox of volume v at the interface, yields

$$\epsilon_d(\omega)+\epsilon_m(\omega)=0 \qquad (2)$$

as the condition for the nontrivial solution which allows the existence of a finite electric field at the boundary. If the frequency dependent dielectric function of the metal $\epsilon_m(\omega)$ is known, Eq. (2) can be solved by assuming the dielectric function of the insulator to be frequency independent, and equal to the optical dielectric constant $[\epsilon_d(\omega)=\epsilon_{do}]$. For a simple free-electron metal, with $\epsilon_m(\omega)=1-\omega_p^2/\omega^2$, we then get $\omega_s=\omega_p/\sqrt{\epsilon_{do}+1}$. If the dielectric is simply the vacuum, then this reduces to the well known result $\omega_s=\omega_p/\sqrt{2}$, which is the relation between the bulk (ω_p) and the surface (ω_s) plasmon frequency of the metal. For Ag metal, however, the dielectric function cannot simply be derived from a Drude-like model, because of the interband transitions from Ag $4d$ to higher lying conduction band states. The net effect of these transitions is to shift the plasmon energy from the value $\hbar\omega_p=9.2$ eV, as calculated in the free-electron limit, to $\hbar\omega_p=3.9$ eV. Instead, using the experimentally measured[21] frequency dependent Ag dielectric function as shown in Fig. 7, we can now solve graphically the Eq. (2). For the vacuum/Ag(100) interface, $\epsilon_{do}=1$ gives a surface plasmon energy of about 3.7 eV, a value that differs by less than 0.2 eV from the bulk value, as also measured by optical experiments.[24] For the MgO(100)/Ag(100) interface, taking the bulk MgO optical constant $\epsilon_{do}=3.01$,[25] we get $\hbar\omega_s=3.2$ eV, which is in excellent agreement with the value of $\hbar\omega_s=3.3$ eV as measured in the EELS experiment on the 20 ML MgO(100)/Ag(100) sample. For the NiO/Ag(100) interface, using the optical constant $\epsilon_{do}=5.43$,[26] we obtain $\hbar\omega_s=2.84$ eV, which is also in very good agreement with the EELS and the Ag $3d$ core level experiments on a 20 ML NiO(100)/Ag(100) sample, where the Ag surface plasmon was indeed found at 3.0 eV.[27] Realizing that Eq. (2), in principle, holds only for the interface between two ideal semi-infinite dielectric media, the agreement indicates that a

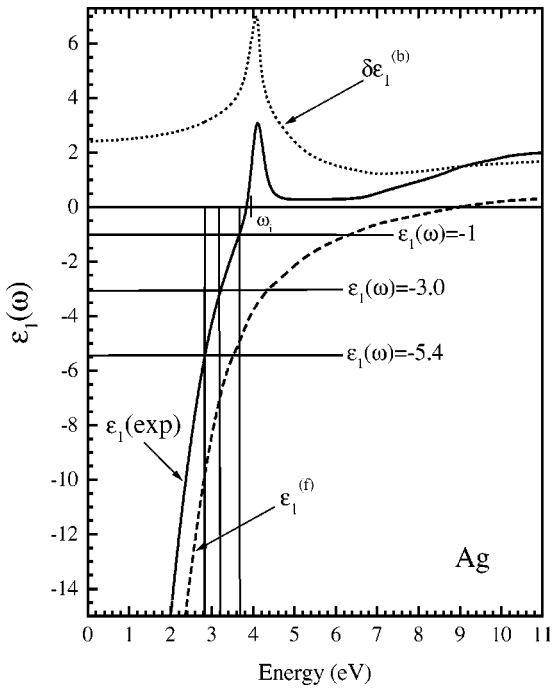

FIG. 7. Real part of the experimental frequency dependent dielectric function of Ag [$\epsilon_1(\omega)$, solid line] and its decomposition into free-electron ($\epsilon_1^{(f)}$, dashed line) and bound-electron ($\delta\epsilon_1^{(b)}$, dotted line) contributions, from Ref. 21. Surface normal modes at the vacuum/Ag, MgO/Ag, and NiO/Ag interface exist for $\epsilon_1(\omega)$ equal to the negative of the optical dielectric constants of vacuum (1), MgO (3.0, Ref. 25), and NiO (5.4, Ref. 26), i.e., with surface-plasmon energies $\hbar\omega_s$ of 3.7 eV, 3.2 eV, and 2.8 eV, respectively.

20 ML film is thick enough to develop the full dielectric properties of the bulk material and to make the effect of the oxide/vacuum interface on the electric–field lines at the oxide/Ag(100) interface completely negligible.

It is worth noting that metal plasmon peaks show up not only in the Ag spectra, but also in the XPS and Auger spectra of the insulating overlayers, with consistently identical energies. These plasmons can be either excited by the electric field associated with a photoelectron traveling through the metal (*extrinsic* plasmons), or coupled to the potential of a suddenly created core hole (*intrinsic* plasmons).[28,29] Both the extrinsic and the intrinsic plasmon peaks will occur at the same energy positions and, although the intensity distribution will be slightly different, it is in general quite difficult to separate the intrinsic from the extrinsic component. However, the plasmon satellites observed in the spectra of the MgO(100) monolayer on Ag(100) are expected to be predominantly intrinsic, because most of the electrons contributing to the spectra have not traveled into the Ag substrate. Support for this expectation can be found from the fact that the plasmon satellites in the Auger spectrum are more intense than in the XPS spectrum. This is based on the idea that, in the linear response regime, the intrinsic plasmon intensity should be four times larger in an Auger experiment (two holes) than in an XPS experiment (one hole), while the extrinsic plasmon intensity should be the same. Moreover, the presence of intrinsic metal surface plasmon excitations in the core level spectra of MgO(100) thin films on Ag(100) is not completely unexpected. In fact, after the emission of a photoelectron or an Auger electron from metals and adsorbates on metal surfaces, the conduction band electrons move in to screen the core hole via collective excitations, resulting in a shift of the threshold energy and the simultaneous appearance of multiple plasmon peaks.[30–33]

The presence of these plasmon peaks in the XPS and Auger spectra of the MgO(100) film on Ag(100) is important to our purposes, because it allows to discriminate between different screening mechanisms possibly responsible for the extra-atomic relaxation energy enhancement observed in MgO(100) thin films on Ag(100).[11] In fact, charge fluctuations on one atom can be screened out by a nearby metal substrate in two possible ways: by transferring electrical charge to a higher lying atomic orbital,[34,35] or by the induced charges localized at the metal surface.[30–33] In both cases, the energy cost of charge fluctuations in the vicinity of the metal is efficiently reduced. It is also very difficult to predict *a priori* which of the two screening channels will prevail. However, if intrinsic surface plasmon peaks show up in the core level spectra of the overlayer, then the dynamical response of the metal to charge excitations in the overlayer can be properly described in terms of image charges, because the latter can be expressed as a superposition of surface charge density fluctuations, which, in the long wavelength limit, are just surface plasmons.[30–33] Therefore, the presence of intrinsic metal surface plasmon peaks in the core level spectra of the oxide thin film on the metal is a direct evidence of the image potential screening of charge fluctuations at oxide-metal interfaces.

It may appear surprising that energy reductions as large as several eV (Ref. 11) are associated with plasmon excitations having very weak spectral intensity. Nevertheless, the energy of these weak structures weighted with their intensity determines the Koopmans theorem[36] average binding energy and the total relaxation energy via well known sum rules,[37–39] so that weak peaks lying at high energy may result in a large value of the relaxation energy, and a consequently large shift of the core level threshold. We remark, however, that the energy cost of charge fluctuations and the changes with film thickness are actually a result of the competition between image potential screening and atomic polarizability. In the monolayer case, for example, the energy loss due to the reduced coordination and the energy gain due to the presence of the metal surface are about 7 eV and 9 eV, respectively,[11] yielding an effective increase of the overall relaxation energy by about 2 eV.[11]

V. CONCLUSIONS

We have analyzed the dynamical response of the Ag(100) metal surface to electronic excitations within supported MgO(100) thin films. We have found the presence of *intrinsic* metal surface plasmon peaks in the core level spectra of the MgO(100) thin films. This provides a direct evidence of image potential screening of charge fluctuations at oxide-metal interfaces.

ACKNOWLEDGMENTS

We would like to thank A. Heeres, J. C. Kappenburg, and H. J. Bruinenberg for their skillful technical assitance. We would like to acknowledge L. Venema for providing the Ag(100) single crystal and M. Mulder for the reflection high-energy electron diffraction gun used for the film thickness calibration. This work was supported by the Netherlands Foundation for Fundamental Research on Matter (FOM) with financial support from the Netherlands Organization for the Advancement of Pure Research (NWO). S.A. acknowledges financial support by the European Union under Contract No. ERBCHBGCT930415. The research of L.H.T. has been made possible by financial support from the Royal Netherlands Academy of Arts and Sciences, as well as the Deutsche Forschungsgemeinschaft through Grant No. SFB 608.

[1] D.M. Duffy and A.M. Stoneham, J. Phys. C **16**, 4087 (1983).
[2] A.M. Stoneham and P.W. Tasker, J. Phys. C **18**, L543 (1985).
[3] A.M. Stoneham and P.W. Tasker, Philos. Mag. B **55**, 237 (1987).
[4] M. W. Finnis, A. M. Stoneham, and P. W. Tasker, in *Metal Ceramic Interfaces*, edited by M. Rühle, A. G. Evans, M. F. Ashby, and J. P. Hirth, Acta/Scripta Metallurgica Proceeding Vol. 4 (Pergamon, Oxford, 1991), p. 35.
[5] M.W. Finnis, Surf. Sci. **241**, 61 (1991).
[6] M.W. Finnis, R. Kashner, C. Kruse, J. Furthmuller, and M. Scheffler, J. Phys. C **7**, 2001 (1995).
[7] D.M. Duffy, J.H. Harding, and A.M. Stoneham, Philos. Mag. A **67**, 865 (1993).
[8] D.M. Duffy, J.H. Harding, and A.M. Stoneham, J. Appl. Phys. **76**, 2791 (1994).
[9] D.M. Duffy, J.H. Harding, and A.M. Stoneham, Acta Metall. Mater. **43**, 1559 (1995).
[10] D.M. Duffy, J.H. Harding, and A.M. Stoneham, Acta Metall. Mater. **44**, 3293 (1996).
[11] S. Altieri, L.H. Tjeng, F.C. Voogt, T. Hibma, and G.A. Sawatzky, Phys. Rev. B **59**, R2517 (1999).
[12] M. Cini, Solid State Commun. **24**, 681 (1977); Phys. Rev. B **17**, 2788 (1978).
[13] G.A. Sawatzky, Phys. Rev. Lett. **39**, 504 (1977).
[14] V.E. Henrich, G. Dresselhaus, and H.J. Zeiger, Phys. Rev. Lett. **36**, 158 (1976).
[15] V.E. Henrich, G. Dresselhaus, and H.J. Zeiger, Phys. Rev. B **22**, 4764 (1980).
[16] D.M. Roessler and W.C. Walker, Phys. Rev. **159**, 733 (1967).
[17] P.A. Cox and A.A. Williams, Surf. Sci. **175**, L782 (1986).
[18] M.C. Wu, C.M. Truong, and D.W. Goodman, Phys. Rev. B **46**, 12 688 (1992).
[19] V.E. Henrich and L.R. Kurtz, J. Vac. Sci. Technol. **18**, 416 (1981).
[20] P.R. Underhill and T.E. Gallon, Solid State Commun. **43**, 9 (1982).
[21] H. Ehrenreich, and H.R. Philipp, Phys. Rev. **128**, 1622 (1962).
[22] R.A. Pollak, L. Ley, F.R. McFeely, S.P. Kowalczyk, and D.A. Shirley, J. Electron Spectrosc. Relat. Phenom. **3**, 381 (1974).
[23] S. Altieri, L.H. Tjeng, and G.A. Sawatzky, Phys. Rev. B **61**, 16 948 (2000).
[24] H. Raether, Springer Tracts Mod. Phys. **38**, 84 (1965).
[25] J.R. Jasperse, A. Kahan, J.N. Plendl, and S.S. Mitra, Phys. Rev. **146**, 526 (1965).
[26] R.J. Powell and W.E. Spicer, Phys. Rev. B **2**, 2182 (1970).
[27] S. Altieri, L. H. Tjeng, A. Tanaka, F. C. Voogt, O. Rogojanu, T. Hibma, and G. A. Sawatzky (unpublished).
[28] J-J. Chang and D.C. Langreth, Phys. Rev. B **8**, 4638 (1973).
[29] W.J. Pardee, G.D. Mahan, D.E. Eastman, R.A. Pollak, L. Ley, F.R. McFeely, S.P. Kowalczyk, and D.A. Shirley, Phys. Rev. B **11**, 3614 (1975).
[30] G.E. Laramore and W.J. Camp, Phys. Rev. B **9**, 3270 (1974).
[31] J. Harris, Solid State Commun. **16**, 671 (1975).
[32] J.W. Gadzuk, Phys. Rev. B **14**, 2267 (1976).
[33] A. Datta and D.M. Newns, Phys. Lett. **59A**, 326 (1976).
[34] N.D. Lang and A.R. Williams, Phys. Rev. B **16**, 2408 (1977).
[35] K. Schönhammer and O. Gunnarsson, Solid State Commun. **23**, 691 (1977).
[36] T. Koopmans, Physica (Amsterdam) **1**, 104 (1934).
[37] B.I. Lundqvist, Phys. Kondens. Mater. **9**, 236 (1969).
[38] D.C. Langreth, Phys. Rev. B **1**, 471 (1970).
[39] J.W. Gadzuk, J. Electron Spectrosc. Relat. Phenom. **11**, 355 (1977).